Discrete element modelling of a masonry wall subjected to shear with taking into account the damage of blocks

Ali BOUKHAM[1] , Thomas PARENT[1], Stéphane MOREL[1], Frederic DUBOIS[2], Jean-Christophe MINDEGUIA[1]

[1] I2M, UMR 5295, Univ. de Bordeaux, Bordeaux, France

[2] LMGC, CNRS, Univ. Montpellier, Montpellier, France

ABSTRACT The masonry structures represent a remarkable portion of the French and world built heritage. The preservation of these buildings requires a multidisciplinary diagnostic approach that includes a structural assessment to estimate their stability. However, this task remains difficult because of the high non linearity of the masonry material and the complexity of the geometries of this type of buildings. For this, several robust modeling strategies have been developed. Among these strategies, block based models based on the discrete element method and more specifically the NSCD (Non Smooth Contact Dynamics) allow to take into account the actual texture of masonry. However, in this type of approach, blocks are elastic and non linearity appears only at the interfaces between blocks governed by cohesive frictional laws. In this study, a new hybrid approach is proposed. It consists in integrating a model combining damageworld-builtcity in finite element blocks. The validation of this numerical approach is carried out on the basis of an experimental campaign on masonry walls tested in shear and subjected to vertical loading.

Keywords Masonry, Damage, NSCD, DEM, FEM

I. INTRODUCTION

Masonry is one of the oldest construction techniques still used today. This technique includes any construction method based on the principle of stacking blocks. The variety of masonry types is due to the diversity of materials (blocks and mortar joints) and methods of arranging blocks during different eras, that differ from one region to another. In fact, construction techniques of masonry have often changed over time to meet specific needs. This historical and diversity aspects of masonry make that a great part of the cultural heritage consists of monumental masonry structures such as towers, castles, churches, mosques, temples, etc.

In recent years, many historical masonry buildings were damaged either due to weathering, fire incidents or earthquakes. These incidents can have drastic consequences either humanly, culturally or financially. In 2019, the famous Notre Dame cathedral of Paris, which is considered as one of the symbols of France, was hit by a devastating fire. As a consequence, the whole timber roof was burned and a part of the stone vaults collapsed. Thus, the preservation and restoration of such buildings requires a multidisciplinary diagnostic approach that includes a structural assessment to estimate their stability. However, the heterogeneity, anisotropy and strong non-linearity of masonry make this task complex. It is even more complicated when historical monuments presents a complex geometry as well as a complex loading history. Hence it is necessary to develop robust numerical modeling strategies dedicated to masonry structures.

Several modelling strategies exist in the literature and can be separated into four major families (D'Altri et al. (2019)) : block based models with or without joints, continuous models where masonry is considered as a homogeneous continuous material, macro-models that model the structure by a system of panels with a non-linear mechanical response and geometry-based models that consider the structure as a rigid solid and assume that the masonry has a infinite compressive strength, a zero tensile strength and prohibition of block's sliding (this approach uses only the geometric and loading data of the structure).
Among the block based models, the NSCD (Non Smooth Contact Dynamics) is one of the discrete element methods developed to model the dynamics of a set of distinct bodies (rigid or deformable) in interaction (Dubois & Jean (2006)). The particularity of this method compared to other discrete element methods is the implicit time integration, the implicit resolution of the contact problem and the possibility of taking into account non regular contact laws. Thus, several NSCD-based modeling strategies can be adapted for masonry structures.
The work presented here is based on the work initially carried out to model the mechanical behaviour of masonry walls under shear Venzal (2020). In this previous study, a simplified approach based on the NSCD was implemented. The masonry was modelled as a stack of homogenized isotropic extended elastic blocks. The stiffness of the mortar joints was integrated in the blocks using linear homogenization. The interaction between these extended blocks is described by a frictional cohesive contact law called FCZM (Venzal (2020)). This frictional cohesive law is adapted to model the mechanical response of the block mortar interface. It takes into account the progressive damage of the interface in tensile (Mode I), shear (Mode II) and tensile-shear mixed mode. In addition, in the case of a load that combines compression and shear, this model allows to gradually take into account friction depending on the damage evolution. The identification of the mechanical parameters of this FCZM law was carried out by means of an experimental characterization campaign using a direct tensile test on masonry duos and a compression/ shear test on masonry triplets.
The validation of this numerical approach was carried out by comparing the experimental results of a masonry wall tested in shear and subjected to vertical loading with the numerical results. In this previous study, it was shown that by directly injecting the parameters of limestone blocks and stone-mortar interfaces identified experimentally, the numerical model does not allow to reproduce directly (i) the experimental horizontal stiffness of the wall and (ii) the failure mechanisms observed experimentally. The modulus of elasticity of the homogenized block was therefore reduced by 86% in order to obtain the experimental stiffness of the wall. In addition, the failure mechanisms were numerically obtained through the introduction of an initial interface damage.
The limitation of this approach is its inability to reproduce the damage of the blocks which is often observed in masonry buildings and typically in walls subjected to shear due to the high compressive stresses. Neglecting this aspect can highly impact the mechanical response of the masonry wall. Thus, it is necessary to model the blocks with a non linear damage model rather than a simple linear elastic one. Also, homogenization of such non linear models is a difficult challenge. To overcome both issues, a novel modelling approach is proposed in this work where masonry is modelled by a stacking of non extended ,non-homogenized and non linear blocks (a model combining damage and plasticity is used for the blocks), that is, keeping their own dimensions and their own material properties. The normal and tangential elastic behaviour of the mortar joint is considered by adding a linear spring to the FCZM law (in both normal and tangential directions).

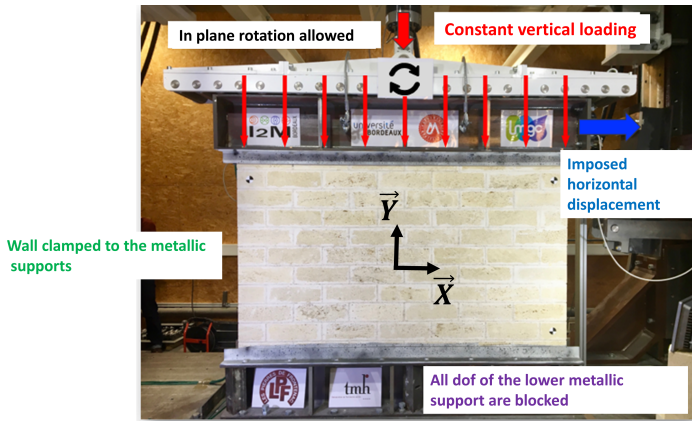

FIGURE 1. Boundary conditions applied to the wall. Venzal (2020)

II. Experimental results

The purpose of this section is to summarize the results of the experimental program conducted by Venzal (2020) on masonry walls subjected to compressive/shear loading.

A. Experimental program

In this previous work, 9 walls were tested under compressive/shear loading. Three different compressive stresses (0.3MPa, 0.4MPa and 0.5MPa) were applied (three walls for each compressive stress) to quantify its impact on the wall behaviour.
The walls were $1,85m$ wide, $1.2m$ tall and $0.15m$ thick and were composed of 11 courses. They were made of soft limestone collected from Frontenac quarry. The selected mortar was a natural hydraulic lime mortar often used in ancient masonry building restoration. For the binder and the sand, NHL3.5 as well as a 0/2mm sand were used. A 1.5 : 1 : 6.5 formulation ("water : binder : sand" expressed in mass ratios) was chosen to optimize the workability of the mortar.
For the boundary conditions, the wall was glued to two metallic supports using an epoxy resin. The lower metallic support was clamped while the upper metallic support's out-of-plane rotation and displacements were blocked. The vertical loading was first applied and then an horizontal displacement was imposed. The displacement and deformation field were measured using stereo correlation. (Figure 1)

B. Experimental results

The experimental results shows that all the 9 walls presents a similar mechanical response. The curves "$F_x - U_x$" of all the walls, where U_x is the applied horizontal displacement while F_x is the corresponding horizontal reaction force, have the same shape (Figure 2). In fact, three different phases can be distinguished on these curves. First, a linear phase is observed which means that the wall is still not damaged and no plastic deformation is yet developed. This first phase is followed by a non linear phase where F_x keeps increasing, the non linearity is caused by the crack's initiation and propagation at the block-mortar interfaces (cracks (a) and (b) in figure 3). The cracking pattern developed in this phase highly depends on the applied compressive stress and on the dispersion of the mechanical properties of the different block-mortar interfaces as will be discussed further in the paper. The last observed phase is characterized by a sharp decrease in F_x due to the crushing of the blocks highly loaded in compression caused by the decrease of the effective

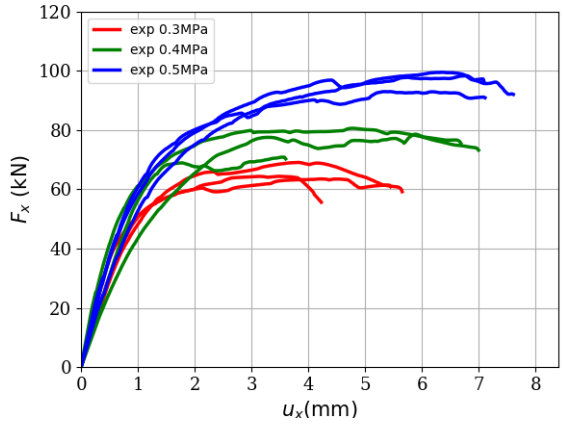

FIGURE 2. The mechanical response $F_x - U_x$ of the tested walls for the three applied compressive stresses. (Venzal (2020))

surface resisting to the normal load.
Another important observation is that the higher the applied compressive stress the higher the failure load. This is explained by the fact that the frictional stresses at the level of the block-mortar interface are more important for higher compressive stresses. Also, since friction contributes more than cohesion to the internal forces, the wall resists to higher forces when the normal loading is higher. However, the stiffness of the wall is not impacted by the normal loading since at finite displacements the contribution of friction is not yet predominant (we recall that the frictional stresses at the interfaces depends on the damage evolution).
For the failure mechanisms, two main mechanisms are observed (Figure 3). In the first one, the horizontal crack (a) is initiated at the lower left corner at the level of the horizontal interface (where the tensile stresses are the highest due to maximal flexural moment at the wall base) and then it propagates horizontally along the interfaces until it reaches the lower right corner (3a). This latter mechanism is observed for low applied compressive stresses. For higher compressive stresses a second mechanism is rather observed. Similarly the horizontal crack (a) initiates at the lower left corner at the level of the horizontal interface and then propagates horizontally for a short distance along the interfaces where it stops propagating due to the high compressive stresses (the high compressive stresses make it hard for the crack to propagates further). At this stage, another diagonal crack (b) initiates at the vertical interface in the middle of the wall where shear and tensile stresses are the highest and then propagates to form a stair-step crack along the diagonal. Also, in this second mechanism the lower right block is damaged in compression (c) (Figure 3b).

III. Numerical results

This section aims to present the novel modelling approach and its validation by comparing the numerical results to the experimental ones.

A. Modelling approach

The proposed approach is a 3D simplified micro modelling approach based on the so-called "non smooth contact dynamics method" or *NSCD* (Dubois & Jean (2006)). In view of the discontinuous character of the masonry formed by a stacking of blocks, this numerical approach has advantages over others modelling

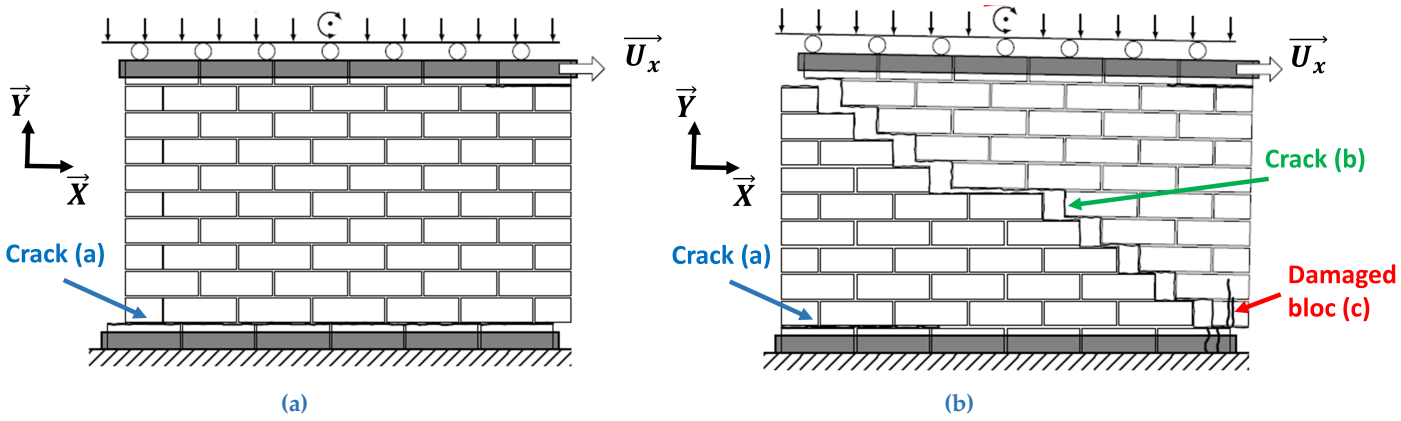

FIGURE 3. Failure mechanisms of the tested walls : (a) for high applied compressive stresses (b) for low applied compressive stresses. (Venzal (2020))

methods given its ability to capture physical phenomena occurring locally at the block/mortar interfaces. The masonry is modelled here by a stacking of non-extended and non-homogenized blocks (keeping their own dimensions and mechanical properties). The mortar and the block/mortar interface is modelled by an interface with an initial gap (Figure 4). The contact law of this interface includes then the mechanical behaviour of both mortar and the block/mortar interface. This is achieved by adding an elastic spring law in both normal and tangential directions to a cohesive frictional law called FCZM (Figure 5).
The stress-seperation law ($\sigma_I - \delta_I$) law in mode I is defined by the following equations :

$$\text{Mode I - tension } (\delta_I \geq 0) \begin{cases} \delta_I = \delta_I^{coh} + \delta_I^{spring} \\ \sigma_I = \sigma_I^{coh} = (1 - d_{coh}) K_I^{coh} \delta_I^{coh} = \sigma_I^{spring} = (1 - d_{spring}) K_I^{spring} \delta_I^{spring} \\ d_{coh} = max_{history}(max(1 - \dfrac{\sigma_I^e}{K_I^{coh} \delta_I^{coh}} e^{\phi_I (\frac{\sigma_I^e}{K_I^0} - \delta_I^{coh})}; 0)) \end{cases} \tag{1}$$

$$\text{Mode I - compression } (\delta_I < 0) \begin{cases} \delta_I = \delta_I^{spring} \ (\delta_I^{coh} = 0) \\ \sigma_I = \sigma_I^{coh} = \sigma_I^{spring} = (1 - d_{spring}^I) K_I^{spring} \delta_I^{spring} \end{cases} \tag{2}$$

Where δ_I the total normal opening of the interface, δ_I^{spring} the normal opening of the elastic spring, δ_I^{coh} the normal opening of the FCZM law, $\sigma_I = \sigma_I^{coh} = \sigma_I^{spring}$ the actual normal stress of the total law which is the same for the normal spring and FCZM law (we recall that the elastic spring and the FCZM law are mounted in series), d_{coh} is the damage variable of the cohesive part that can only increase, d_{spring} is a constant value chosen to calibrate the normal stiffness of the elastic spring (it can be seen as a parameter reproducing the observed difference between the stiffness of the mortar at the scale of the specimen and of the structure), ϕ_I a parameter computed to ensure that the dissipated energy is equal to G_{f_I} : $\int_0^\infty \sigma_I^e e^{\phi_I (\delta_I^e - \delta_I^{coh})} \, d\delta_I^{coh} = G_{f_I}$ and $(\sigma_I^e, K_I^{coh}, K_I^{spring}, G_{f_I})$ are the input parameters of the law in mode I defining respectively the elastic limit stress $[Pa]$, the FCZM stiffness $[Pa/m]$, the spring stiffness $[Pa/m]$ and the cohesive energy $[J/m^2]$.

For mixed mode shear+compression, the stress-sliding law ($\sigma_{II} - \delta_{II}$) is defined by the following set of equations :

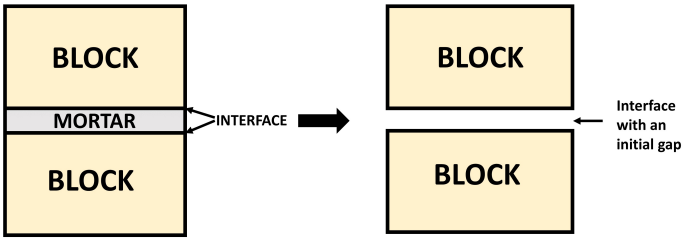

FIGURE 4. **The modelling approach adapted for masonry.**

FIGURE 5. **Rheological model of the proposed contact law : (a) in mode I (b) in mode II.**

$$\text{Mode II - shear/compression} \begin{cases} \delta_{II} = \delta_{II}^{coh} + \delta_{II}^{spring} \\ \sigma_{II} = \sigma_{II}^{FCZM} = \sigma_{II}^{coh} + \sigma_{\mu} = \sigma_{II}^{spring} \\ \sigma_{II}^{spring} = (1 - d_{spring}) K_{II}^{spring} \delta_{II}^{spring} \; ; \sigma_{II}^{coh} = (1 - d_{coh}) K_{II}^{coh} \delta_{II}^{coh} \\ |\sigma_{\mu}| \leq \sigma_{\mu_c} = \mu d^p |\sigma_N| \\ d_{coh} = max_{history}(max(1 - \dfrac{\sigma_{II}^e}{K_{II}^{coh} \delta_{II}^{coh}} e^{\phi_{II}(\frac{\sigma_{II}^e}{K_{II}^{coh}} - \delta_{II}^{coh})}; 0)) \end{cases} \tag{3}$$

In a similar way to mode I, δ_{II} the total tangential sliding of the interface, δ_{II}^{spring} the tangential sliding of the elastic spring, δ_{II}^{coh} the tangential sliding of the FCZM law, $\sigma_{II} = \sigma_{II}^{FCZM} = \sigma_{II}^{spring}$ the actual tangential stress of the total law which is the same for the tangential spring and FCZM law, σ_{μ} the frictional stress of the FCZM law, σ_{μ_c} the sliding frictional stress that depends on the damage value, d_{coh} is the damage variable that can only increase, d_{spring} is a constant value chosen to calibrate the tangential stiffness of the elastic spring, ϕ_{II} a parameter computed to ensure that the dissipated energy is equal to $G_{f_{II}}$: $\int_0^{\infty} \sigma_{II}^e e^{\phi_{II}(\delta_{II}^e - \delta_{II}^{coh})} \, d\delta_{II}^{coh} = G_{f_{II}}$, σ_N is the compressive stress applied and $(\sigma_{II}^e, K_{II}^{coh}, K_{II}^{spring}, G_{f_{II}}, p, \mu)$ are the input parameters of the law in mode II defining respectively the elastic limit stress $[Pa]$, the FCZM stiffness $[Pa/m]$, the spring stiffness $[Pa/m]$, the cohesive energy $[J/m^2]$, the exponent of the frictional stress evolution and the coefficient of friction.

As the relation $\sigma_i - \delta_i \; ; i \in \{I, II\}$ is implicit, a non linear solver is used to determine σ_i given a certain value of δ_i. In tension, an exponential cohesive law is used for the FCZM law (1). While in compression, a signorini law is used since a physical interface have no stiffness in compression (2). For this reason, the stiffness of the total law in compression is the same as of the elastic spring. Also there is no damage evolution in compression. While for shear+compression mode, the FCZM law considers that the shear stress is the sum of an exponential cohesive stress (mode II) and frictional stress, where this latter increase with the evolution of d (3). Figure 6 illustrates the mechanical response of this contact law in both pure mode I and

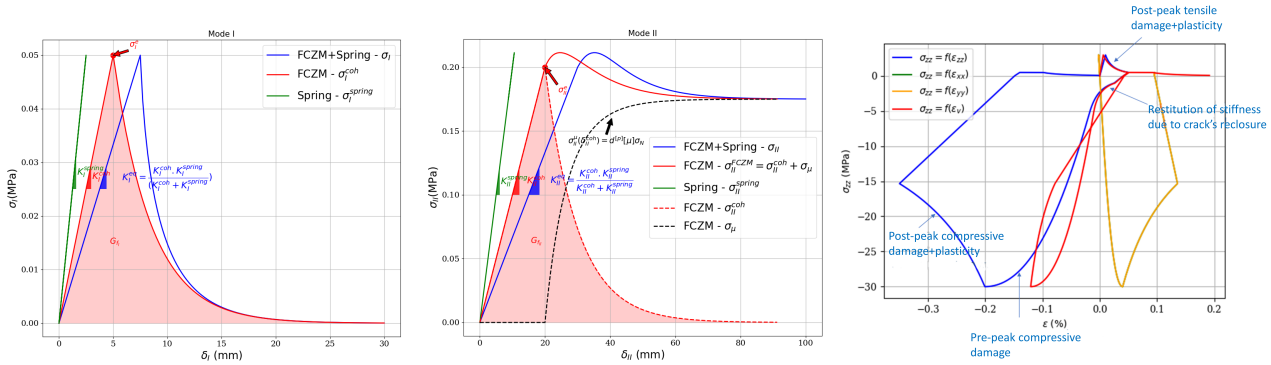

(a) (b) (c)

FIGURE 6. Mechanical response of the proposed contact law : (a) in mode I (b) in mode II. And the ENDO3D model response under a uniaxial tensile/compression test along z axis : (c).

TABLE 1. ENDO3D parameters

Elasticity		Tensile			Compression				
E (Pa)	ν	R_t (Pa)	ε_{pic_t}	G_{f_t} (J/m^2)	R_c (Pa)	ε_{pic_c}	δ	β	ε_{kdc}

in compression/shear mode.

For the blocks, a model called "ENDO3D" coupling damage and plasticity is used (Morenon et al. (2022)). Specifically, this model is suitable to model the mechanical behaviour of natural stones since it is capable of capturing the asymmetric response in tension/compression, dilatancy, energy regularization in tension and cracks reclosure in compression. This is achieved by incorporating a multi-surface plasticity approach and different damage tensors for tension and compression. Figure 6c illustrates the mechanical response of the ENDO3D model in the case of a cube (modeled by one finite element) subjected to a uniaxial tensile/compression load. The main model parameters are summarized in table 1.
Finally, the proposed contact law as well as the damage-plasticity model were added to the discrete element software `LMGC90`.

B. Numerical wall model

In `LMGC90` software the 3D geometry of the masonry wall was created by using the simplified micro modeling technique. Masonry units were meshed using cubic elements (2 elements along x,y axes and one element along z axis), while the mortar and block/mortar interface were modeled by a 2D contact elements with an initial gap (4 contact points by contact element). The number of mesh elements and of contact points were determined in order to optimize time calculation while preserving accurate results. Rigid elements were used to model the upper and lower metallic supports. Figure 7 displays the discrete element model of the masonry wall with the corresponding block's finite element meshes and contact points.
Boundary conditions similar to the experiments used experimentally are applied to the numerical model. The blocks of the first and last courses are glued to the metallic supports through a coupled dof contact law. For the load history, gravity, normal loading and imposed horizontal displacement were applied successively and gradually using tangent hyperbolic functions (to avoid sudden variations that can lead to dynamic effect).

(a) (b)

FIGURE 7. Numerical model of the wall : (a) wall mesh (b) contact points.

TABLE 2. ENDO3D parameters used

Elasticity		**Tensile**			**Compression**				
E (GPa)	ν	R_t (MPa)	ε_{pic_t}	G_{f_t} (J/m^2)	R_c (MPa)	ε_{pic_c}	δ	β	ε_{kdc}
11.1	0.2	1	0.9009×10^{-4}	60	9.46	0.13×10^{-1}	0.4	0.2	0.18×10^{-1}

Concerning the material's parameters, they were taken from (Bisoffi-Sauve (2016), Parent (2015),Venzal (2020)). Tables 2 and 3 regroup the different parameters used for the damage-plasticity model and for the contact law model.

C. Numerical results

The numerical results of the model with non linear blocks show a good agreement with the experimental ones (Figure 8a). In fact, using the initial parameters shown in table 3 (with a $d_{spring} = 0$) the numerical model was unable to reproduce the correct horizontal wall stiffness ($\approx 71kN/mm$) nor the observed failure mechanisms. To obtain the correct stiffness, an isotropic damage (isotropic means here that same damage value is considered for both normal and tangential directions) $d_{spring} = 0.953$ is applied on the elastic spring part of the contact law (representing the mortar). While the stiffness is correctly captured by the numerical model, the failure mechanisms are still not correctly reproduced. To overcome that, an initial damage $d_{coh} = 0.99944$ (this damage value leads to a 60% decrease of σ^e_{II}) is considered for the frictional cohesive part of the contact law (representing the block/mortar interface). In fact, this initial damage allowed to reproduce the observed failure mechanisms without impacting the horizontal wall stiffness. This reduction of the mechanical properties of the contact law identified at the scale of the specimen is certainly explained by the different curing and drying conditions of the grouted mortars at the wall's scale compared to the specimen's scale.

However, even though the same parameters previously set are used for the model with linear blocks. The corresponding numerical results do not agree with the experimental ones (Figure 8b). This highlights the fact that the elastic linear hypothesis is not suitable for extreme load cases where the blocks are highly damaged. In fact, the failure of the lower right block of the wall in compression impacts the initiation of failure mechanisms of the wall as well as its mechanical response (Figure 9a). Also, unexpectedly tensile damage

TABLE 3. Law contact (FCZM+spring) parameters used

Linear spring		**FCZM (mode I)**			**FCZM (mode II)**		
K_I^{spring} (Pa/m)	K_{II}^{spring} (Pa/m)	σ^e_I (MPa)	K_I^{coh} (Pa/m)	G_{f_I} (J/m^2)	σ^e_{II} (MPa)	K_{II}^{coh} (Pa/m)	$G_{f_{II}}$ (J/m^2)
4.3×10^{11}	1.8×10^{11}	0.05	1.21×10^{11}	3	0.27	2.8×10^{11}	206

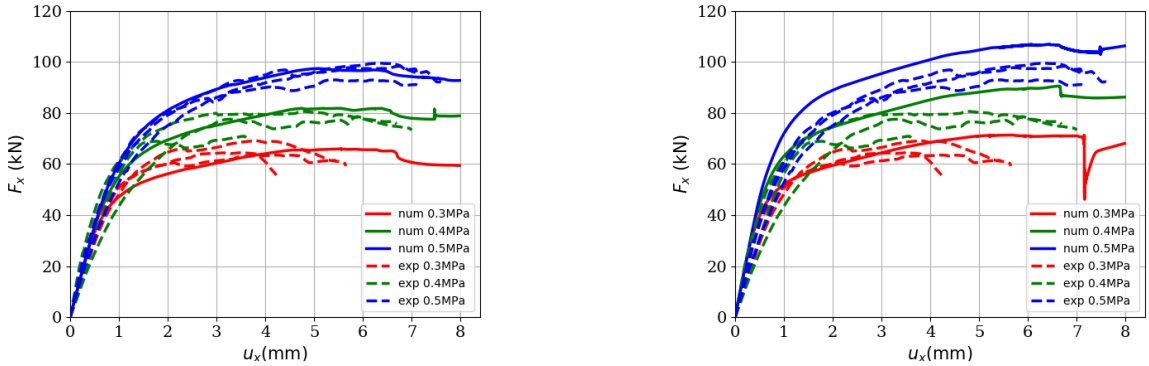

FIGURE 8. Comparison of the numerical results and experimental results in terms of F_x-U_x curves : (a) blocks with a damage-plasticity model (b) blocks with an linear elastic model.

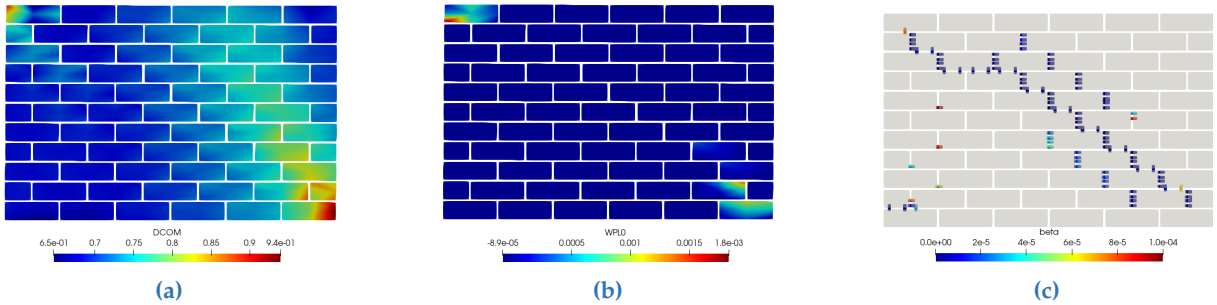

FIGURE 9. Different damage fields of the numerical wall with nonlinear blocks at ($\sigma_N = 0.5MPa$; $U_x = 8mm$): (a) compressive damage in the blocks (b) tensile cracks opening (c) interface damage.

is also observed but only in some fewer blocks. For that reason, the model with linear blocks gives incorrect results both in terms of stiffness and failure loads (the pre-peak damage in compression impacts the stiffness of the wall). Nevertheless, both models capture the cracks at the contact interfaces. Figures 10c and 9c shows the highly damaged interfaces (at the contact points), and it can be seen that the same crack patterns observed experimentally are reproduced.

IV. Conclusions and perspectives

In this work, a new modelling strategy is developed in which damage can initiates in both interfaces and blocks. This new approach, allows to capture all the typical failures mechanisms of a masonry. Also, since the appropriate mechanical parameters found experimentally are put in the blocks and the interface+interface/block assembly, no homogenization step is needed. This is achieved by introducing a new contact law in which a normal and a tangential elastic spring is added to a frictional cohesive model which allows to model the interface+interface/block assembly separately.

The necessity of taking into account the damage in blocks was highlighted by comparing the numerical results of two wall models (with non linear blocks and with only linear elastic blocks). It was shown, that the linear model gave results different from the experimental ones. However, it was possible to obtain better re-

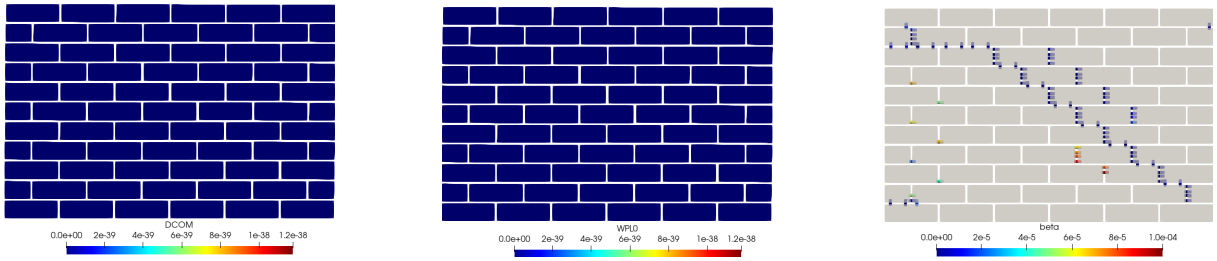

(a) (b) (c)

FIGURE 10. Different damage fields of the numerical wall with linear elastic blocks ($\sigma_N = 0.5MPa$; $U_x = 8mm$): (a) compressive damage in the blocks (b) tensile cracks opening (c) interface damage.

sults with the linear model but with a different set of parameters than the one used in the non linear model. But this can lead to a false parameters setting and can highly impact the results of larger scale models (at the scale of a cathedral, tower, castle...). Also, the damage in blocks is predominant in masonry structures as was seen for the shear wall, which limits the use of the discrete model with linear blocks.
In the scope of this work, an experimental campaign is planned to properly characterize the mechanical behaviour of the materials used in the tested walls. Also, the sensitivity analysis of the wall's numerical response with respect to the different model's parameters is still to be done to have a better understanding of the main causes triggering the failure mechanisms of the tested walls. Finally, this modelling approach will be applied on the cathedral of Notre Dame of Paris.

References

Bisoffi-Sauve, M. (2016), Etude des ouvrages maçonnés en pierre par la méthode des éléments discrets : caractérisation et modélisation du comportement cohésif des joints, Theses, Université de Bordeaux.
URL: *https://tel.archives-ouvertes.fr/tel-01373072*

D'Altri, A., Sarhosis, V., Milani, G., Rots, J., Cattari, S., Lagomarsino, S., Sacco, E., Tralli, A., Castellazzi, G. & Miranda, S. (2019), 'Modeling strategies for the computational analysis of unreinforced masonry structures: Review and classification', *Archives of Computational Methods in Engineering* **27**.
URL: *https://link.springer.com/article/10.1007/s11831-019-09351-x*

Dubois, F. & Jean, M. (2006), *The non smooth contact dynamic method: recent LMGC90 software developments and application*, Springer Berlin Heidelberg, Berlin, Heidelberg, pp. 375–378.
URL: *https://doi.org/10.1007/3-540-31761-9*$_4$4

Morenon, P., Sellier, A. & Domède, N. (2022), 'Computational performances optimization of a non-linear mechanical behaviour model for geomaterials', *Academic Journal of Civil Engineering* **40**(1), 207–210.
URL: *https://journal.augc.asso.fr/index.php/ajce/article/view/3115*

Parent, T. (2015), Méthodologie de Diagnostic de Structures Maçonnées Anciennes, Theses, Université Toulouse 3.
URL: *https://tel.archives-ouvertes.fr/tel-01403780*

Venzal, V. (2020), Modélisation discrète du comportement mécanique desouvrages maçonnés en pierre. Aspects expérimentaux - Analyse énergétique, Theses, Université de Bordeaux.
URL: *https://tel.archives-ouvertes.fr/tel-03003557*